Supporting Information

In Situ Time-Resolved Attenuated Total Reflectance Infrared Spectroscopy for Probing Metal-Organic Framework Thin Film Growth

Junjie Zhao,[†‡§] Berc Kalanyan,[‡§*] Heather F. Barton,[†] Brent A. Sperling,[‡] Gregory N. Parsons[†*]

[†] Department of Chemical & Biomolecular Engineering, North Carolina State University, 911 Partners Way Campus Box 7905, Raleigh, NC 27695, United States. (gnp@ncsu.edu)
[‡] National Institute of Standards and Technology (NIST), Gaithersburg, MD, 20899, United States. (berc.kalanyan@nist.gov)

([§]JZ and BK contributed equally to this work)

Experimental

Atomic Layer Deposition of ZnO on Si Wafers:

50 mm diameter double-side polished Si(111) wafers (undoped, float-zone, Virginia Semiconductor Inc.) were used as received. ZnO thin films were deposited on the Si wafers using atomic layer deposition (ALD) as described previously.[1] Si wafers were horizontally placed in a custom-built flow tube ALD reactor kept at 100 ℃. The pressure during the deposition was controlled at ≈ 3.5 mm Hg. Diethyl zinc (95 %, Strem Chemicals) and deionized water were sequentially dosed to the reactor for 0.2 s, with 30 s of N_2 (99.999 %, Airgas, passed through a purifier) purging between each precursor dose. The number of ALD cycles ranged from 100 to 500 for the investigation of the effect of ZnO thickness. The growth rate of ALD ZnO was found to be ≈ 0.20 nm/cycle by ellipsometry (Alpha-SE, J.A. Woollam Co.).

Liquid flow cell with in situ ATR-FTIR:

Figure S1 schematically shows the liquid flow cell reactor and the associated optics configured for ATR-FTIR mode. For each measurement, a whole Si wafer (50 mm diameter) was used as the internal reflection element (IRE). The wafer was positioned in a recessed aluminum pedestal. Square pockets were cut out at two opposing edges of the pedestal and were fitted with Ge right-angle prisms (12.7 mm sides, ISP Optics, Irvington, NY). The wafer was coupled with the prisms by mechanical clamping using #6-80 screws with 2 mm ball tips. A mid-IR spectrometer (Digilab FTS 7000, Agilent Technologies, Santa Clara, CA) with a globar source was used for the FTIR measurements. Collimated light from the bench was focused onto face of the first Ge prism by a 90 ° off-axis parabolic (OAP) mirror (50 mm effective focal length). Once through the first Ge prism, the IRE, and the second Ge prism, light was re-collimated by a second OAP mirror (50 mm effective focal length) and directed by a plane mirror into a reflective Schwarzschild objective, which focused the beam onto a

cryogenic HgCdTe (MCT) detector (Model 997-0054, InfraRed Associates, Inc., Stuart, FL). An o-ring sealed custom-made PTFE flow cell (~0.6 mL internal volume) was mounted on top of the wafer substrate, whose inlet was connected to a peristaltic pump (MasterFlex L/S, Cole-Parmer, Vernon Hills, IL) by flexible tubing (fluoropolymer, 1.6 mm inner diameter). The outlet tubing for the flow cell was connected with the waste bottle.

Study of HKUST-1 Thin Film Formation by HDS Conversion:

All reagents were prepared using H_2O/EtOH as the solvent (ethanol volume fraction of 0.5), abbreviated as "mixed solvent". 500 mL of 300 mmol/L $Cu(NO_3)_2$ solution was prepared by dissolving 36.24 g of $Cu(NO_3)_2 \cdot 3H_2O$ (99 % - 104 %, Sigma-Aldrich) in mixed solvent. 1 L of 10 mmol/L H_3BTC was prepared by dissolving 2.10 g of trimesic acid (95 %, Sigma-Aldrich) in mixed solvent. Reactant solutions of other concentrations used in this study were prepared in a similar manner. After the ALD ZnO coated Si IRE was loaded into the flow cell, a reference FTIR spectrum was first collected while mixed solvent was continuously pumped into the cell. The flow rate was kept at 100 mL/min for all experiments. Next, time-resolved ATR-FTIR spectra were recorded and simultaneously processed by removing the solvent background during the flow of reactant solutions. In a typical experiment, $Cu(NO_3)_2$ solution was first pumped into the flow cell for 120 s, followed by a solvent flush using mixed water/ethanol for 60 s. Next, H_3BTC solution was pumped into the cell for 300 s. After a final purge step with mixed water/ethanol for 120 s, acquisition of spectra was stopped. The flow cell was further purged and dried with N_2 gas (feed pressure: ≈ 0.8 bar) for 10 min before the wafer was removed from the cell for analysis. The deposited MOF thin films were imaged by optical microscopy (Leica DMLM, Leica Microsystems, Wetzlar, Germany) and scanning electron microscopy (SEM) (FEI Verios 460L, FEI Company, Hillsboro, OR). All samples were sputter-coated with a thin Au/Pt layer before SEM imaging to mitigate surface charging. X-ray diffraction (XRD) was performed on a

Rigaku SmartLab diffractometer (Rigaku Corporation, Tokyo, Japan).

Kinetic Modeling of HDS Formation from ZnO

The Beer-Lambert law can be written for ATR-FTIR spectroscopy in a differential form:[2–4]

$$dI_z = -\varepsilon C I_z dz \tag{S1}$$

where I_z is the intensity of the evanescent wave at a propagation distance of z from the IRE surface, ε is the molar attenuation coefficient (in units of m^2/mol), and C (in units of mol/m^3) is the concentration of the functional groups corresponding to the IR band.

The decay of electric field strength (E_z) is given as a function of the propagation depth from the IRE surface:[5,6]

$$E_z = E_0 e^{-\gamma z} \tag{S2}$$

where γ is defined as the reciprocal of the penetration depth, and is depended on the refractive indices of the IRE (n_1) and the thin film on top of the IRE (n_2), the incident angle (θ) and the IR wavelength (λ).

$$\gamma = \frac{1}{d_p} = \frac{2\pi n_1 \sqrt{sin^2\theta - \left(\frac{n_2}{n_1}\right)^2}}{\lambda} \tag{S3}$$

Since the intensity is proportional to the square of the electric field strength, I_z can be described as a function of z with weak absorption assumption:[6]

$$I_z = I_0 e^{-2\gamma z} \tag{S4}$$

Substitution of Equation S1 with Equation S4 yields

$$dI_z = -\varepsilon C I_0 e^{-2\gamma z} dz \tag{S5}$$

So the decrease of intensity after one total reflection is given

$$\Delta I = -\int_0^\infty \varepsilon C I_0 e^{-2\gamma z} dz \tag{S6}$$

For the reaction that forms (Zn,Cu) HDS from an ALD ZnO thin film, we understand that the topmost portion of the ZnO film is converted to HDS first, resulting in a ZnO/HDS

bilayer. Equation S6 then becomes

$$\Delta I = -\int_0^{d_{ZnO}} \varepsilon C I_0 e^{-2\gamma z} dz - \int_{d_{ZnO}}^{d_{HDS}} \varepsilon C I_0 e^{-2\gamma z} dz - \int_{d_{HDS}}^{\infty} \varepsilon C I_0 e^{-2\gamma z} dz \quad \text{(S7)}$$

where d_{ZnO} and d_{HDS} are the distances from the IRE surface to the top surface of the ZnO film and the HDS film, respectively. The three segments of integration range represent the absorption in the ZnO layer, in the HDS layer, and in the solution. Because the concentration of NO_3^- groups in the initial ZnO layer is negligible, the first integral reduces to zero:

$$\int_0^{d_{ZnO}} \varepsilon C I_0 e^{-2\gamma z} dz = 0 \quad \text{(S8)}$$

Assuming the concentration of NO_3^- groups in the HDS film and in the solution is uniform, with values of $C_{N,HDS}$ and $C_{N,Sol}$ holding constant, we obtain

$$\Delta I = -\varepsilon C_{N,HDS} I_0 \int_{d_{ZnO}}^{d_{HDS}} e^{-2\gamma z} dz - \varepsilon C_{N,Sol} I_0 \int_{d_{HDS}}^{\infty} e^{-2\gamma z} dz \quad \text{(S9)}$$

which reduces to

$$\Delta I = \frac{\varepsilon C_{N,HDS} I_0}{2\gamma} (e^{-2\gamma d_{HDS}} - e^{-2\gamma d_{ZnO}}) - \frac{\varepsilon C_{N,Sol} I_0}{2\gamma} e^{-2\gamma d_{HDS}} \quad \text{(S10)}$$

Or

$$\Delta I = \frac{\varepsilon C_{N,HDS} I_0}{2\gamma} e^{-2\gamma d_{ZnO}} (e^{-2\gamma L_{HDS}} - 1) - \frac{\varepsilon C_{N,Sol} I_0}{2\gamma} e^{-2\gamma d_{ZnO}} e^{-2\gamma L_{HDS}} \quad \text{(S11)}$$

In this expression, L_{HDS} is the thickness of the HDS film, *i.e.* $L_{HDS} = d_{HDS} - d_{ZnO}$. During the initial period of reaction on ZnO, $L_{HDS}/d_p << 1$.

$$e^{-2\gamma L_{HDS}} \approx 1 - 2\gamma L_{HDS} \quad \text{(S12)}$$

So

$$\Delta I = -\varepsilon C_{N,HDS} L_{HDS} I_0 e^{-2\gamma d_{ZnO}} + \varepsilon C_{N,Sol} L_{HDS} I_0 e^{-2\gamma d_{ZnO}} - \frac{\varepsilon C_{N,Sol} I_0}{2\gamma} e^{-2\gamma d_{ZnO}} \quad \text{(S13)}$$

Or

$$\Delta I = -\varepsilon I_0 e^{-2\gamma d_{ZnO}} \left(C_{N,HDS} L_{HDS} + \frac{C_{N,Sol}}{2\gamma} - C_{N,Sol} L_{HDS} \right) \quad \text{(S14)}$$

$$\frac{\Delta I_N}{I_0} = -N\alpha \left[\frac{C_{N,Sol}}{2\gamma} + (C_{N,HDS} - C_{N,Sol}) L_{HDS} \right] \quad \text{(S15)}$$

where N is the number of total reflections, ΔI_N is the intensity change after N total reflections,

and α is defined as

$$\alpha = \varepsilon I_0 e^{-2\gamma d_{ZnO}} \tag{S16}$$

Absorbance (A) is defined as:

$$A = -log_{10}\left(\frac{I}{I_0}\right) \tag{S17}$$

Or

$$A = -\frac{1}{ln10}\, ln\left(1 + \frac{\Delta I_N}{I_0}\right) \tag{S18}$$

With weak absorption assumption, $\Delta I \ll I_0$, resulting in the approximation

$$A \approx -\frac{1}{ln10} \cdot \frac{\Delta I_N}{I_0} \tag{S19}$$

So

$$A = \frac{N\alpha}{ln10}\left[\frac{C_{N,Sol}}{2\gamma} + (C_{N,HDS} - C_{N,Sol})L_{HDS}\right] \tag{S20}$$

Assuming the initial ZnO-to-HDS conversion follows pseudo-first order kinetics with constant $Cu(NO_3)_2$ concentration on the ZnO surface during continuous flow, we obtain L_{HDS} as a function of time:

$$L_{HDS} = \frac{k_{app} C_{Cu} t \cdot V}{C_{N,HDS} \cdot S} \tag{S21}$$

where k_{app} is the apparent rate constant (in units of min^{-1}), t is the reaction time (in units of min), C_{Cu} (mol/m^3) is the concentration of Cu^{2+} in the solution, V (m^3) is the volume of $Cu(NO_3)_2$ solution involved in the reaction, and S (m^2) is the geometric area of the HDS film, *i.e.* the planar surface area on the wafer exposed to reactants and defined by the o-ring seal.

Absorbance is therefore related to reaction time:

$$A = \frac{N\alpha}{ln10} \cdot \frac{C_{N,Sol}}{2\gamma} + \frac{N\alpha}{ln10} \cdot \frac{(C_{N,HDS} - C_{N,Sol})C_{Sol}}{C_{N,HDS}} \cdot \frac{kV}{S} \cdot t \tag{S22}$$

Or

$$A = \frac{N\alpha}{ln10} \cdot \frac{C_{N,Sol}}{2\gamma} + \frac{(C_{N,HDS} - C_{N,Sol})C_{Sol}}{C_{N,HDS}} \cdot \varphi t \tag{S23}$$

where k_{app} is the apparent rate constant and is defined as

$$\varphi = \frac{N\alpha}{ln10} \cdot \frac{k_{app}V}{S} \quad \text{(S24)}$$

Equation S20 appears in the main article text as Equation 1, Equation S16 as Equation 2, Equation S3 as Equation 3, Equation S23 as Equation 5, and Equation S24 as Equation 6.

Kinetic Modeling of MOF Formation from HDS

Similar to the derivation for S7, we obtain the following equation to describe the intensity change of the evanescent wave during the conversion of HDS to HKUST-1:

$$\Delta I = -\int_0^{d_{HDS}} \varepsilon' C' I_0 e^{-2\gamma' z} dz - \int_{d_{HDS}}^{d_{MOF}} \varepsilon' C' I_0 e^{-2\gamma' z} dz - \int_{d_{MOF}}^{\infty} \varepsilon' C' I_0 e^{-2\gamma' z} dz \quad \text{(S25)}$$

where d_{MOF} is the distance from the IRE surface to the top surface of the MOF film, ε' is the molar attenuation coefficient (in units of m^2/mol) for carboxylate groups, C' is the concentration of carboxylate groups, γ' is the reciprocal of the penetration depth during this reaction. Because the concentration of carboxylate groups in the initial HDS layer is negligible, the first integration reduces to zero. We also found that contributions from the solution to the measured absorbance can be neglected, since flowing H_3BTC solution over a bare IRE (spectra referenced against Si) produces no detectable bands in the carboxylate region. So Equation S25 can be further simplified to

$$\Delta I = -\varepsilon' C_{C,MOF} I_0 \int_{d_{HDS}}^{d_{MOF}} e^{-2\gamma' z} dz \quad \text{(S26)}$$

where $C_{C,MOF}$ is the concentration of carboxylate groups in the MOF film. With an approximation similar to that used in Equation S12, Equation S26 can be further reduced to

$$\Delta I = -\varepsilon' I_0 e^{-2\gamma' d_{HDS}} C_{C,MOF} L_{MOF} \quad \text{(S27)}$$

where L_{MOF} is the thickness of the HKUST-1 MOF film. So $\nu_{as}(OCO^-)$ absorbance A' is given as

$$A' = \frac{N\alpha'}{ln10} C_{C,MOF} L_{MOF} \quad \text{(S28)}$$

$$\alpha' = \varepsilon' I_0 e^{-2\gamma' d_{HDS}} \quad \text{(S29)}$$

Assuming that the initial reaction to form HKUST-1 MOF from HDS follows first order kinetics with a constant H_3BTC concentration on the HDS surface during flow, we obtain L_{MOF} as a function of time:

$$L_{MOF} = \frac{k'_{app} C_{BTC} t \cdot V'}{C_{C,MOF} \cdot S'} \quad \text{(S30)}$$

where k' is the rate constant (in units of min^{-1}) for the reaction that converts HDS to HKUST-1, t is the reaction time (in units of min), C'_{sol} (mol/m^3) is the concentration of H_3BTC in the solution, V' (m^3) is the volume of H_3BTC solution involved in this reaction, and S' (m^2) is the geometric area of the MOF film. Substituting S28 with S30, we obtain

$$A' = \frac{N\alpha'}{ln10} \frac{k'_{app} V'}{S'} C_{BTC} t \quad \text{(S31)}$$

Or

$$A' = \varphi' C_{BTC} t \quad \text{(S32)}$$

where φ' is defined as

$$\varphi' = \frac{N\alpha'}{ln10} \frac{k'_{app} V'}{S'} \quad \text{(S33)}$$

Equation S32 appears in the main article text as Equation 8, and Equation S33 as Equation 9.

Analysis of Time-Resolved ATR-FTIR Spectra

Integrated peak areas for time-resolved FTIR spectra were calculated using the OPUS software package (version 7.2, Bruker Corporation, Billerica, MA). A linear baseline was used for each IR band, with the baseline endpoints determined by taking the arithmetic average of absorbance values from approximately 100 wavenumbers on either side of the band of interest. Error in the integrated peak areas are a function of spectral signal-to-noise ratio (S/N) and the position of the baseline. Spectral S/N was found to vary based on the magnitude of the clamping force applied to the wafer to establish the Si/Ge contact. The clamping force was not regulated for this study, therefore some variation in spectral S/N is

reflected in the integrated area analyses. The sensitivity of the integrated area to endpoints that describe the linear baseline was somewhat mitigated by allowing the software to choose endpoints based on point averaging. For a representative dataset, the root-mean-square (RMS) noise in the spectra was calculated to be <0.01 in absorbance units (a.u.) in the 1700 cm^{-1} to 1550 cm^{-1} range. The RMS S/N value was approximately 3 during reactant flow.

Note about Quantitative Analysis of ATR-FTIR Spectra

During our modeling analysis, we made use of several simplifications and assumptions. However, further development and optimization of the models is needed in the future to incorporate non-ideal factors. In particular, simple analyses based on geometric parameters (angle of incidence, wafer thickness, polarization, *etc.*) may be insufficient to properly describe the measured quantities (*i.e.* absorbance). In the proximity of the coupling pins that ensure contact between the wafer and the prisms, strain apparently induces depolarization, which is difficult to model. Others have also noted that for multiple-reflection ATR accessories that included thin IREs mechanically coupled to prism elements, the absorbance may not directly scale with the number of reflections.[7]

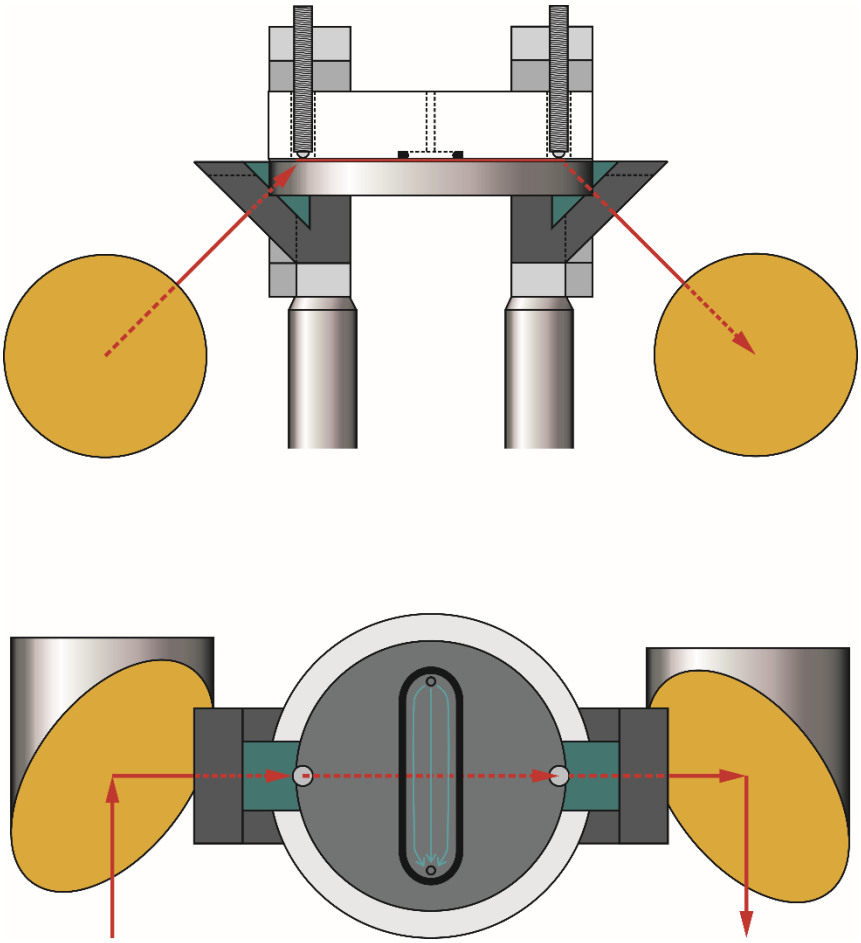

Figure S1. Schematic illustration of the flow-cell ATR-FTIR set-up for investigation of MOF thin film growth.

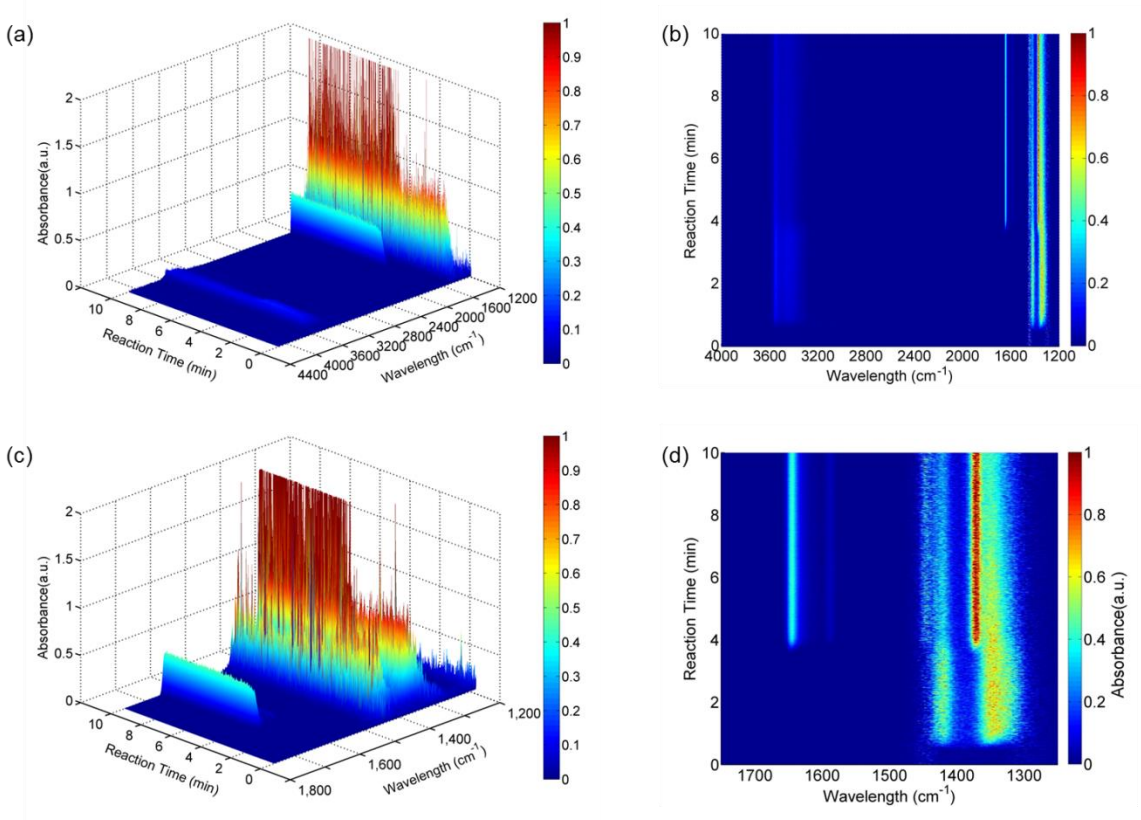

Figure S2. Time-resolved ATR-FTIR spectra collected during the synthesis of HKUST-1 thin films from an ALD ZnO thin film template. The wavelength range in a-b is from 1200 cm^{-1} to 4000 cm^{-1}, while the range in c-d is from 1250 cm^{-1} to 1750 cm^{-1}.

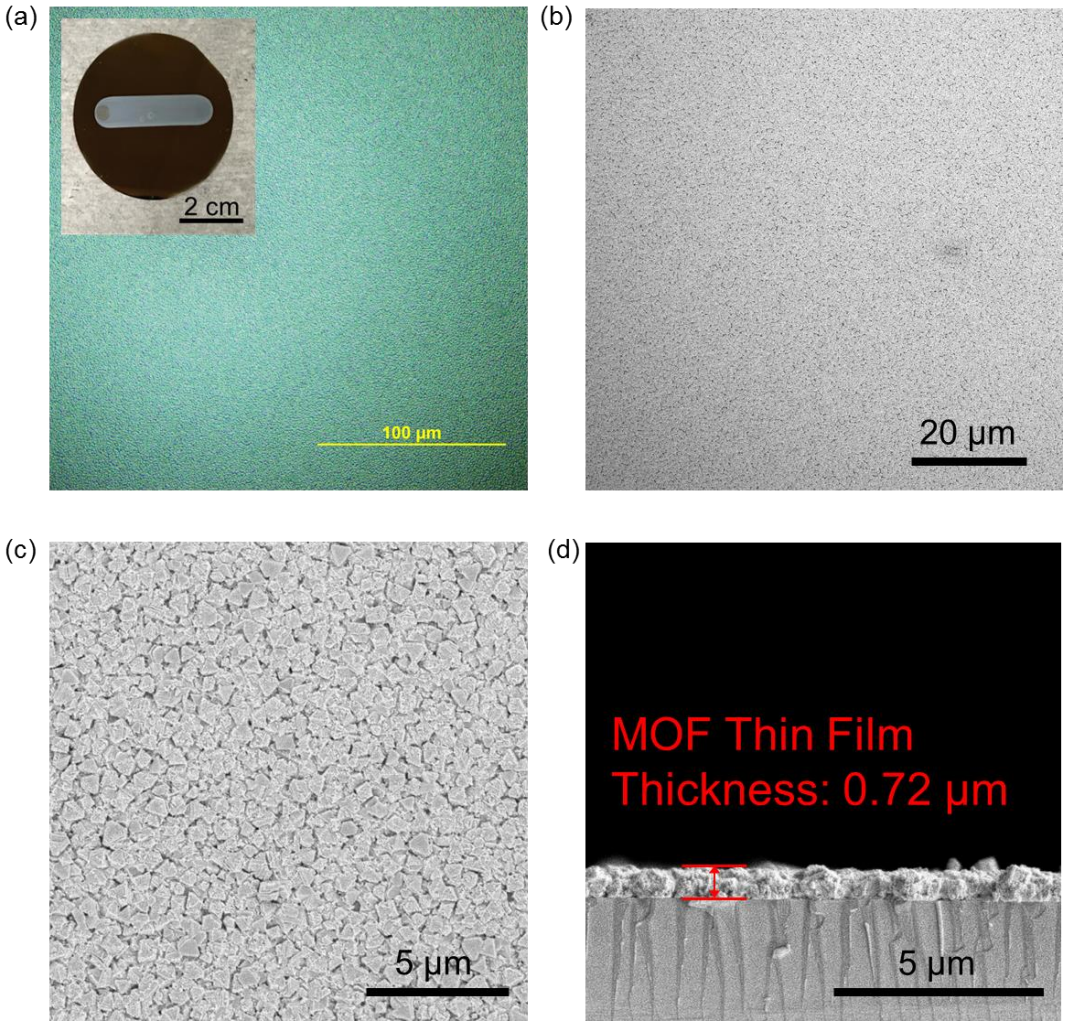

Figure S3. (a) Optical image and (b-d) SEM images of HKUST-1 thin film synthesized by HDS conversion (300 cycles of ALD ZnO as initiation layer) in the flow-cell ATR setup. Inset image in (a) is a photograph showing the MOF thin film formed in the flow channel on a 50 mm wafer.

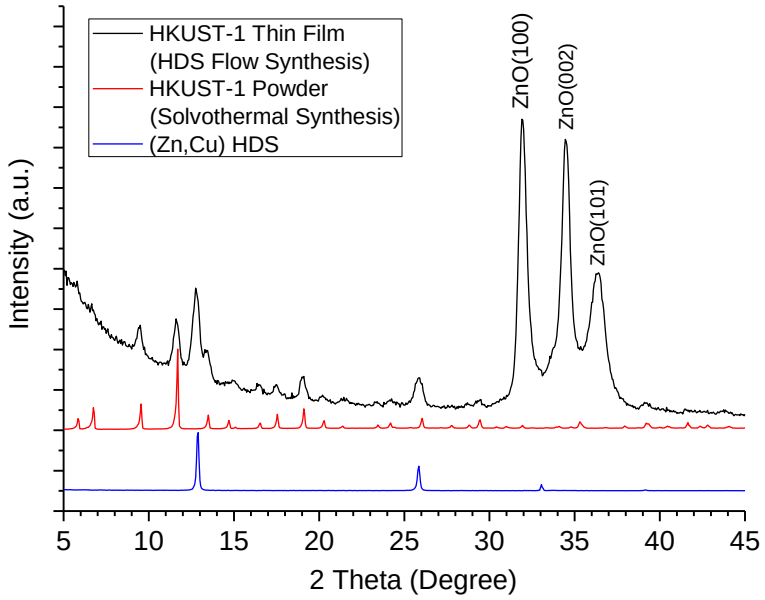

Figure S4. XRD patterns of HKUST-1 thin film synthesized via HDS conversion (300 cycles of ALD ZnO as initiation layer) in the flow-cell ATR setup (black), HKUST-1 powder prepared by solvothermal synthesis (red) and (Zn,Cu) hydroxy nitrate HDS film converted from ALD ZnO (blue). The thin film patterns were measured using glancing incidence XRD, while the powder pattern was measured by powder X-ray diffraction.

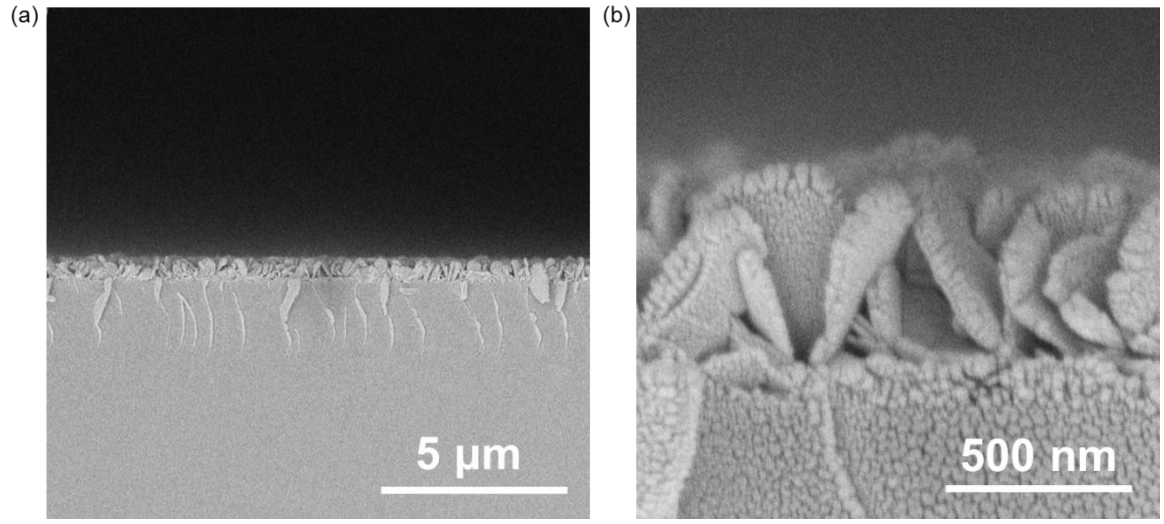

Figure S5. SEM images of (Zn,Cu) HDS thin film converted from the thickest ALD ZnO initiation layer (500 cycles) used in this work. The average thickness of the HDS film is *c.a.* 0.56 µm, which is smaller than the calculated penetration depth of the ATR evanescent wave.

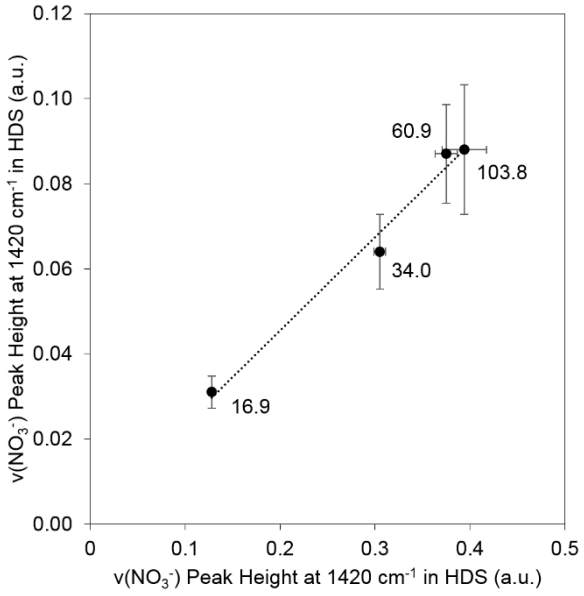

Figure S6. $\nu(NO_3^-)$ peak height measured by transmission FTIR (ordinate) and ATR-FTIR (abscissa) after HDS growth saturation. Thicknesses of the ALD ZnO initiation layers range from 17 nm to 104 nm (indicated by data labels). Transmission and ATR measurements are well correlated and both show signal saturation from (Zn,Cu) HDS grown from sufficiently thick ZnO (greater than 60 nm) initiation layers. This result also indicates that the *in situ* measurements were within the information depth of our ATR-FTIR configuration. Error bars represent the average noise from each FTIR spectrum in the 2200 cm^{-1} to 1600 cm^{-1} range. The dashed line is generated from a linear fit to the data (R^2 = 0.985).

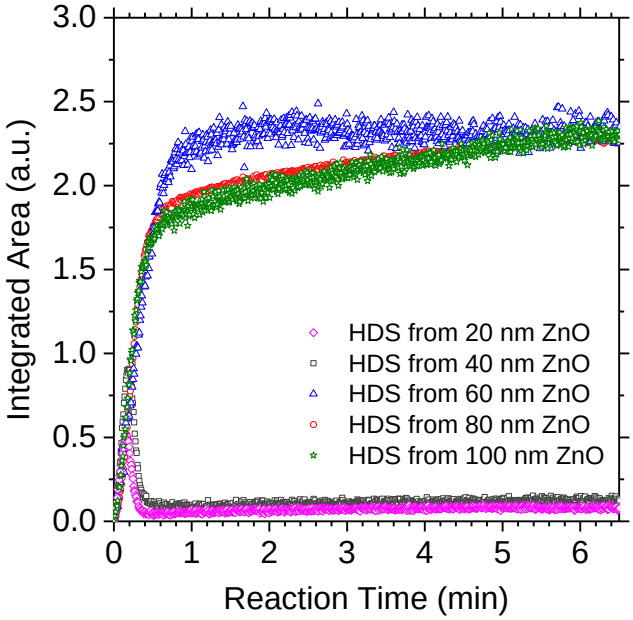

Figure S7. Integrated IR peak area for $\nu_{as}(OCO^{-})$ at ~1647 cm^{-1} as a function of reaction time during the flow of H_3BTC solutions on the (Zn,Cu) HDS films converted from ≈ 20 nm to ≈ 100 nm thick ALD ZnO initiation layers. MOF formation was observed for all HDS surfaces, while delamination occurred for thin HDS films without a ZnO interfacial adhesion layer.

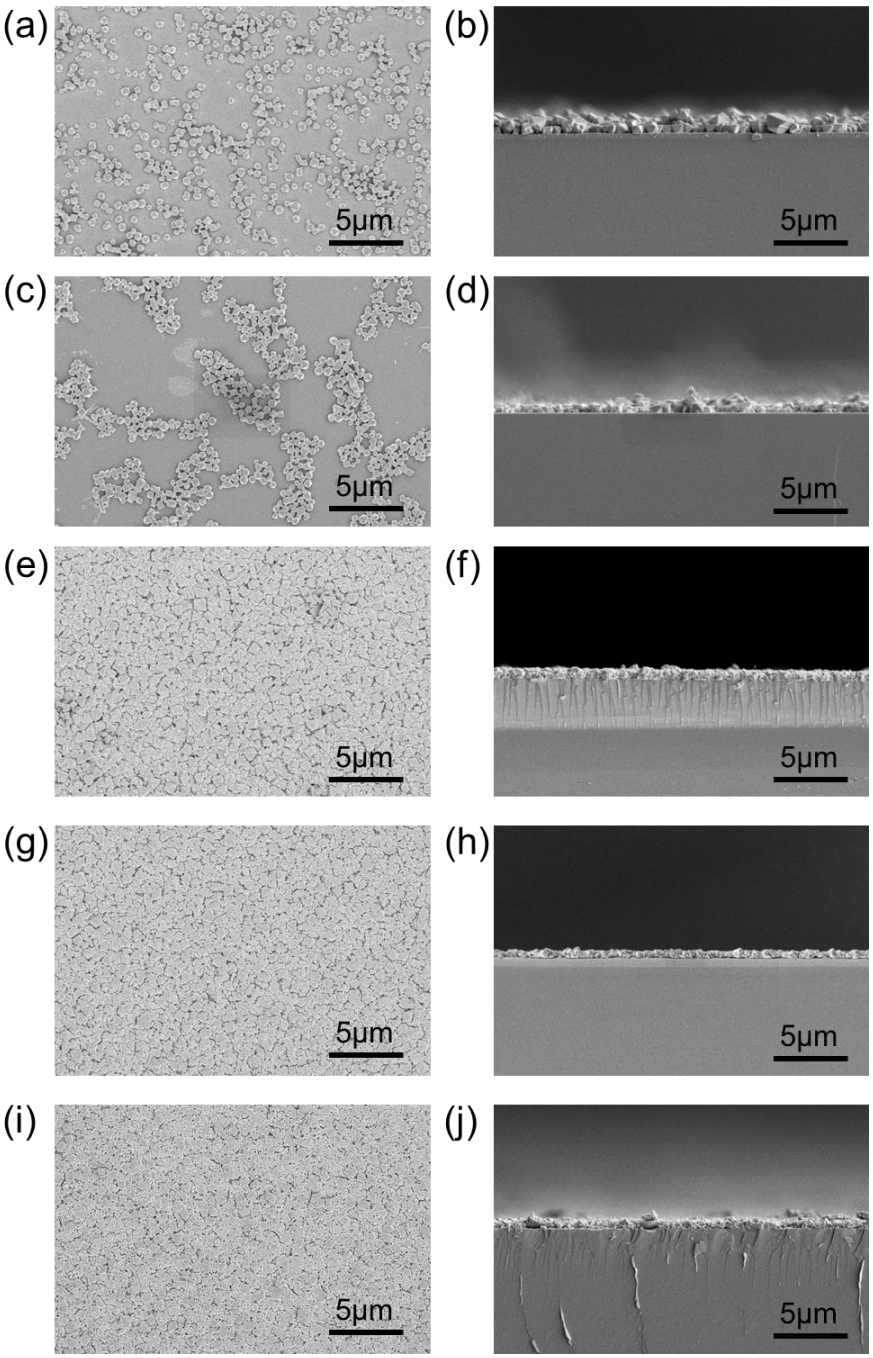

Figure S8. SEM images of HKUST-1 films synthesized by HDS conversion using (a-b) 17.3 nm ± 0.6 nm, (c-d) 34.0 nm ± 0.1 nm, (e-f) 54.8 nm ± 3.7 nm, (g-h) 71.6 nm ± 0.4 nm, and (i-j) 96.1 nm ± 4.7 nm of ALD ZnO initiation layers respectively. Densely packed HKUST-1 films were obtained using thick ZnO (≈ 55 nm to ≈ 96 nm) initiation layers, while film delamination was observed for thin ZnO layers (≈ 17 nm and ≈ 34 nm).

References

(1) Zhao, J.; Nunn, W. T.; Lemaire, P. C.; Lin, Y.; Dickey, M. D.; Oldham, C. J.; Walls, H. J.; Peterson, G. W.; Losego, M. D.; Parsons, G. N. Facile Conversion of Hydroxy Double Salts to Metal-Organic Frameworks Using Metal Oxide Particles and Atomic Layer Deposition Thin-Film Templates. *J. Am. Chem. Soc.* **2015**, *137*, 13756–13759.

(2) Fieldson, G. T.; Barbari, T. A. The Use of FTi.r.-a.t.r. Spectroscopy to Characterize Penetrant Diffusion in Polymers. *Polymer* **1993**, *34*, 1146–1153.

(3) Elabd, Y. A.; Baschetti, M. G.; Barbari, T. A. Time-resolved Fourier transform infrared/attenuated total reflection spectroscopy for the measurement of molecular diffusion in polymers. *J. Polym. Sci. Part B Polym. Phys.* **2003**, *41*, 2794–2807.

(4) Hallinan, D. T.; Elabd, Y. A. Diffusion of Water in Nafion Using Time-Resolved Fourier Transform Infrared−Attenuated Total Reflectance Spectroscopy. *J. Phys. Chem. B* **2009**, *113*, 4257–4266.

(5) Harrick, N. Electric Field Strengths at Totally Reflecting Interfaces. *J. Opt. Soc. Am.* **1965**, *55*, 851-857.

(6) Tompkins, H. G. The Physical Basis for Analysis of the Depth of Absorbing Species Using Internal Reflection Spectroscopy. *Appl. Spectrosc.* **1974**, *28*, 335–341.

(7) Schädle, T.; Mizaikoff, B. Selecting the Right Tool: Comparison of the Analytical Performance of Infrared Attenuated Total Reflection Accessories. *Appl. Spectrosc.* **2016**, *70*, 1072–1079.